NASA TECHNICAL NOTE

NASA TN D-7632

HOLOGRAPHIC AND ULTRASONIC DETECTION OF BOND FLAWS IN ALUMINUM PANELS REINFORCED WITH BORON-EPOXY

by Robert J. Platt, Jr., and Lewis B. Thurston, Jr.

Langley Research Center
Hampton, Va. 23665

NATIONAL AERONAUTICS AND SPACE ADMINISTRATION • WASHINGTON, D. C. • JULY 1974

1. Report No. NASA TN D-7632	2. Government Accession No.	3. Recipient's Catalog No.
4. Title and Subtitle HOLOGRAPHIC AND ULTRASONIC DETECTION OF BOND FLAWS IN ALUMINUM PANELS REINFORCED WITH BORON-EPOXY		5. Report Date July 1974 6. Performing Organization Code
7. Author(s) Robert J. Platt, Jr., and Lewis B. Thurston, Jr.		8. Performing Organization Report No. L-9410 10. Work Unit No. 501-22-03-01
9. Performing Organization Name and Address NASA Langley Research Center Hampton, Va. 23665		11. Contract or Grant No. 13. Type of Report and Period Covered Technical Note
12. Sponsoring Agency Name and Address National Aeronautics and Space Administration Washington, D.C. 20546		14. Sponsoring Agency Code
15. Supplementary Notes		

16. Abstract

An experimental investigation was made of the application of holographic interferometry to the nondestructive detection of unbonded areas (flaws) in bonded panels. Flaw-detection results were compared with results obtained with an ultrasonic flaw detector. For flaws beneath 5 and 10 plies of boron-epoxy, holography, with panel deformation accomplished by a reduction in ambient pressure, is less sensitive than the ultrasonic method, but does have operational advantages.

As part of this investigation, a process for the manufacture of bonded panels, which incorporated known unbonded areas, was developed. The unbonded areas were formed without the use of foreign materials, which should make the method suitable for the construction of reference standards for bonded panels whenever needed for the proper setup of ultrasonic flaw-detection instruments.

17. Key Words (Suggested by Author(s)) Holographic interferometry Ultrasonic flaw detection Unbonded areas Bonded composites	18. Distribution Statement Unclassified – Unlimited STAR Category 15		
19. Security Classif. (of this report) Unclassified	20. Security Classif. (of this page) Unclassified	21. No. of Pages 34	22. Price* $3.25

*For sale by the National Technical Information Service, Springfield, Virginia 22151

HOLOGRAPHIC AND ULTRASONIC DETECTION OF BOND FLAWS IN ALUMINUM PANELS REINFORCED WITH BORON-EPOXY

By Robert J. Platt, Jr., and Lewis B. Thurston, Jr.
Langley Research Center

SUMMARY

An experimental investigation was made of the application of holographic interferometry to the nondestructive detection of flaws, which consisted of airtight unbonded areas within bonded panels. Results of the inspection with a commercial ultrasonic flaw detector were used as a basis for comparison with the holographic results.

As part of the investigation, a process for the manufacture of bonded panels, which incorporated known unbonded areas, was developed. The unbonded areas were formed without the use of foreign materials, which should make the method suitable for the construction of reference standards for bonded panels whenever needed for the proper setup of ultrasonic flaw-detection instruments.

Panel deformation, which was necessary for flaw detection by holography, was performed by static bending, heating, ultrasonic vibration, and by a decrease in ambient pressure. This last method (vacuum deformation) was the most effective, permitting detection of a 0.5-cm-square flaw beneath 5 plies of unidirectional boron-epoxy and a 1.0-cm-square flaw beneath 10 plies. Such detection sensitivity is inferior to that obtainable with an ultrasonic flaw detector, but holography with vacuum deformation does have operational advantages.

INTRODUCTION

Designers of aircraft structures are making increased use of composite materials of high specific strength and stiffness, such as those combining continuous boron or graphite filaments in a resin matrix. Current composite fabrication methods require extensive use of adhesive bonding to join composites to metals or composites to other composites. Flaws may exist in these bonds, or in the composite itself, which could affect the reliability of the structure.

The use of ultrasonic inspection instruments for the detection of these flaws, such as unbonded areas and delaminations, is well established in the aerospace industry. This nondestructive evaluation (NDE) may be performed by probing the structure with a localized beam of ultrasonic energy generated by a transducer and measuring the energy either

reflected from interfaces or transmitted through the structure. Requirements of the method include a liquid couplant between the ultrasonic transducer and the test object, the need to scan the object with the transducer, the proper selection of values for the numerous test parameters that affect the results, and expert operation of the equipment. Because of these requirements, a more easily applied method of flaw detection for bonded construction is needed.

One of the newest methods of NDE is holographic interferometry. This flaw-detection method does not require a liquid couplant or scanning of the object as does the ultrasonic method. Holographic interferometry does require some deformation of the object in order that locally flawed material may be displaced sufficiently with respect to the unflawed material (on the order of a wavelength of light) that these flaws can be detected.

Holographic interferometry, a useful application of optical holography, was discovered several years ago (refs. 1 to 3). As an NDE method, it has been used successfully for the detection of unbonded areas in tires (ref. 4) and in honeycomb panels (refs. 4 to 6). The more difficult problem, that of detection of unbonded areas in test samples of composite-reinforced metal sheet by holographic interferometry, was examined in reference 7. Heat and ultrasonic vibration were used for deformation of the samples. Some success was achieved with the use of vibration, but interpretation of the results was not always straightforward.

The present paper is an extension of the investigation of reference 7 and will further examine the usefulness of holographic interferometry for the detection of unbonded areas in bonded panels. Two additional methods of panel deformation, static bending and ambient pressure change, were investigated. To serve as a basis for comparison with the holographic results, the panels were also inspected with an advanced commercial ultrasonic NDE instrument. As part of this investigation, a unique method was developed for the manufacture of unbonded areas in bonded panels. This method excluded foreign materials which could affect ultrasonic beam transmission through the panels and possibly give false indications with the ultrasonic inspection instrument.

MANUFACTURE OF PANELS

Evaluation of the usefulness of holographic interferometry as an NDE technique required bonded panels containing known defects. The four panels constructed for this purpose are described in table I. Three panels were constructed of unidirectional boron-epoxy composite bonded to aluminum sheet. A fourth panel was constructed of boron-epoxy bonded to boron-epoxy with all filaments unidirectional. Each panel was 20 cm square and incorporated 20 unbonded areas. The planned sizes and locations of these unbonded areas (hereinafter referred to as flaws) are indicated in figure 1(a). The flaws in panels A and B were under 5 and 10 plies of boron-epoxy, respectively; the thickness

of the aluminum alloy approximated the composite thickness in both cases. These two panels acted as a check on detection sensitivity as affected by material thickness. Panel C was constructed of all boron-epoxy (10 plies) to determine if replacement of the metal with composite material affected the detection sensitivity. Panel D was made to investigate the effect of a thicker metal on the detection of flaws under five plies of boron-epoxy.

The method of panel manufacture permitted the sizes and locations of the flaws to be controlled without the inclusion of foreign material. In order to make detection more difficult, the unbonded surfaces contacted each other and the flaws gave no visual indication of their presence. Figure 1(b) is a photograph of the aluminum sheet of panel A with cemented epoxy film patches which formed the flaws. Epoxy cement was used only near the edges of each patch, leaving the inner unbonded area to form the flaw. Each patch was rolled down to remove air bubbles and insure good contact. The sizes of the flaws could not be perfectly controlled because of cement flow during the rolling process, even though most of the cement was scraped away before applying the patch.

The final step in manufacture of a panel was to bond a previously cured 20-cm-square sheet of multiple-ply unidirectional boron-epoxy to the base sheet and its patches. For this last bonding operation, a room-temperature-cure epoxy was used. The adhesive thickness was 0.10 to 0.15 mm.

The epoxy film used for the flaw patches was made especially for this application. Epoxy was pressed between metal blocks covered with polyvinyl fluoride film to prevent adhesion. The resulting epoxy film was cured at about 360 K. Inspection of this film revealed numerous holes caused by small air bubbles. These holes were filled by a second application of epoxy; the film was again pressed between the blocks and cured as before. The finished film was 0.04 to 0.05 mm thick. The epoxy used for this film was identical with that used for the previously described final bonding operation of the panels.

The above method of flaw manufacture introduced no foreign materials which could affect the transmission of ultrasound. For this reason, the method should be suitable for making reference standards for bonded panels whenever needed for the proper setup of ultrasonic flaw-detection instruments.

APPARATUS AND TESTS

Holography

Optical holography is a method for recording the complex wave front received from an object illuminated by coherent light. This recording, usually made on a high resolution photographic plate, is called a hologram. A three-dimensional virtual image of the object may be reconstructed by illuminating the developed hologram with a beam of

coherent light. This image is viewed by looking through the hologram, as through a window, and may be photographed with a camera.

The hologram records both intensity and phase information received from the object. This is done by recording the optical interference at the hologram between the coherent light from the object and a separate coherent reference beam directed at the hologram. Optical holography is discussed in detail in reference 8.

Holographic interferometry.- Optical holography was used for interferometry in three different ways. These and other means of holographic interferometry are described in detail in reference 8. Real-time interferometry was performed by making a hologram of the object, developing it, and replacing it in its original position. The undisturbed object and the hologram were both illuminated by coherent light from a laser. The observer then saw a virtual image of the object superimposed on the real object. Deformation of the object surface created an interference fringe pattern which apparently overlaid the object. These fringes represented lines of equal change of optical path length. A discontinuity in the fringe pattern indicated an abnormal local surface displacement from which was inferred the presence of an underlying flaw.

Double-exposure interferometry required two exposures of the holographic plate with deformation of the object between exposures. The fringe pattern was then fixed in the plate emulsion and could be reconstructed for viewing at any later time.

Time-average interferometry was used when the object was being vibrated to effect deformation. A single exposure of the holographic plate was made, during which the object completed many cycles of vibration. However, much of this time was spent near the maximum amplitude position, which resulted in a fringe pattern weighted toward that position. As with the double-exposure method, the fringe pattern was fixed in the plate emulsion.

Holographic procedures.- The optical arrangement used is shown in figure 2. The holographic system used was the standard off-axis reference beam arrangement (ref. 8), with the addition of a large beam splitter in front of the object. Thus, an observer looking through the hologram views the center of the object along a line which coincides with the laser illumination. A continuous-wave 50-mW He-Ne laser supplied coherent light with a wavelength of 0.6328 μm. The laser beam was divided into an object beam and a reference beam by the first beam splitter. Each beam was filtered and expanded by a spatial filter consisting of a lens and pinhole. Photographs of this equipment, as well as a glass bell jar used for part of this investigation, are shown in figure 3. The table top, constructed with a honeycomb core, was supported by four innertubes for vibration isolation.

Detection of the built-in flaws in a panel by holographic interferometry required that the panel be deformed slightly. Four methods of deformation were tested: static bending, heating, ambient pressure decrease, and ultrasonic vibration.

Deformation by static bending was performed by applying a concentrated load near the center of the panel. The edges of the panel were restrained by a frame which was held in a vise. The holographic plate was exposed at each of two different loads to produce a double exposure.

Deformation by heating was better suited to real-time holography. The panel was heated briefly with a heat gun while being viewed through a previously made hologram. This method depended on the reduction in heat transfer at the flaws to produce local distortions of the surface.

Deformation by ambient pressure decrease was performed by placing the panel in a glass bell jar and making a double-exposure hologram. One exposure was made at atmospheric pressure and another at a reduced pressure. Figure 3 shows the bell jar with a panel in place. Overall panel restraint was provided by a metal backing plate to which the edges of the panel were clamped.

Deformation by vibration at ultrasonic frequencies was performed as described in reference 7. The aim was to resonate the unbonded material of the flaw. If the vibration amplitude of the unbonded material was sufficiently greater than the amplitude of the panel itself, the flaw could be located. Two types of piezoelectric transducers were used to vibrate the panels (ref. 7). The first type of transducer was a small wafer of piezoelectric ceramic material bonded to the metal side of the panel. A sine wave oscillator and amplifier were used to excite the transducer over a wide frequency range. Real-time holographic interferometry was used to detect the frequencies which best resonated unbonded material, but time-average interferometry was used to record the fringe patterns at these frequencies.

Larger vibration amplitudes were possible with the second type of transducer. This transducer was a hollow cylinder of piezoelectric ceramic material with a tapered solid aluminum horn (fig. 4(a)) cemented at one end of the cylinder. The horn acted as an acoustic transformer and was designed to increase the vibration amplitude by a factor of 10 from the transducer to the tip of the horn. Design information for this kind of horn may be found in reference 9. Since this device was effective only near its design frequency, time-average interferometry was used with the horn transducer at its resonant frequency. Transducers of three different lengths, each with a horn of appropriate length, were used. These transducers were most effective at 35, 53, and 67 kHz.

Figure 4 shows a panel ready for vibration deformation with the shortest horn transducer. The panel was clamped along its edges to a frame which was held in a vise. The horn transducer was held against the panel by the transducer support. No couplant was used between the horn and panel. The rearview photograph (fig. 4(a)) shows a horn transducer as well as a bonded transducer mentioned earlier.

To improve the quality of the reconstructed holographic image, the panels were painted on both sides (one side for panel C) with aluminum paint rather than with flat white paint. Light reflected from aluminum paint has a higher component in the specular direction than from flat paint. Since the use of the large beam splitter permitted near-normal illumination and viewing of the panel, it looked brighter and fringe contrast was improved with the aluminum paint.

The large beam splitter introduced a mirror reversal of the image as seen in the hologram reconstruction and as photographed with a camera. This reversal was corrected in the printing process by reversal of the negative.

Ultrasonics

The ultrasonic flaw detector used in this investigation was a modern commercial high resolution instrument designed to generate pulses of broad-band electrical energy over a frequency band of approximately 5 to 50 MHz. This instrument was connected to a piezoelectric transducer, which produced pulses of ultrasonic energy and focused this radiation on the panel being evaluated. Ultrasonic energy pulses reflected from the panel were received by the same transducer and converted to an electrical signal which was displayed on an oscilloscope as signal strength as a function of time (termed A-scan). Both the transducer and panel were immersed in a tank of water to provide a good medium for ultrasonic energy transmission. The instrument and tank are shown in figure 5. An automatic mechanism was mounted above the tank to scan the panel by translation of the transducer. The instrument was provided with gate and sensitivity controls which permitted a particular peak of the reflected energy to be selected to turn on the beam of the B/C-scan storage oscilloscope when the peak amplitude exceeded a preset level (ref. 10). The scanning of this oscilloscope beam was synchronized with the transducer scanning to provide a plan view of the panel (C-scan) on which were indicated the areas of exceptional reflection.

The panels were examined by both the pulse-echo and the auxiliary reflector techniques. With the pulse-echo technique, ultrasonic energy was reflected from either the bond or the back surface and was used to control the writing of the storage beam oscilloscope to provide a C-scan. With the auxiliary reflector technique, ultrasonic energy was reflected from a glass reflector placed behind the panel being evaluated and was used to control the writing of the oscilloscope.

RESULTS AND DISCUSSION

Panel A

Ultrasonic inspection.- The results of four different ultrasonic C-scans of panel A (five-ply boron-epoxy bonded to 0.64-mm-thick aluminum sheet) are shown in figure 6.

These represent the best delineation of flaws for the four possible combinations of the transducer: (1) pulse-echo technique facing the composite side, (2) pulse-echo technique facing the metal side, (3) auxiliary reflector technique facing the composite side, and (4) auxiliary reflector technique facing the metal side. In each case, both of the available focused transducers, designed for frequencies of 2.25 MHz and 15 MHz, were used and the better results are presented in figure 6. By using the pulse-echo technique from the composite side (fig. 6(a)), six of the smallest flaws were not detected and some of the larger flaws were not well defined. Better results were obtained from the metal side (fig. 6(b)), probably because the effects of scattering of the ultrasonic energy by the filaments were avoided.

The signal level used for the C-scans of figures 6(a) and 6(b) did not provide any distinction between the unflawed area of the panel and the background. To indicate the boundaries of the panel, the scan was repeated with increased gain. This second scan produced the widely spaced lines visible in figures 6(a) and 6(b). Two 1.27-cm-square serrated metal blocks are shown in the upper part of each photograph. These blocks were also scanned by the transducer and serve as a scale in the photographs. The distance between scale markings is 2.5 mm on one side of each block and 2.0 mm on the other side.

The best results using the auxiliary reflector technique were obtained with the 15-MHz transducer and are shown in figures 6(c) and 6(d). These figures show that equally good results were obtained with the transducer facing either the composite or the metal side. This technique tends to emphasize any area which impedes the transmission of ultrasonic energy more than a well-bonded area of the panel. Thus, a rectangular piezoelectric wafer and metal foil lead, used for vibrating the panel for a holographic test, are clearly visible at the bottom of figures 6(c) and 6(d) and are indistinguishable from the flaws.

The best results for panel A were obtained using the pulse-echo technique from the metal side (fig. 6(b)). This technique resulted in the most accurate size representation of the built-in flaws and detected even the smallest flaw.

Holographic inspection.- Panel A was examined with holographic interferometry by use of four different methods to obtain panel deformation. Deformations were produced by heating, static bending, ambient pressure decrease, and ultrasonic vibration of the panel. Heating has been used with some success in the past, especially for the detection of unbonded face sheets of honeycomb-core panels (refs. 4 and 5). For the present tests, a heat gun was momentarily directed at each side of panel A and the changing fringe pattern observed. This method proved completely ineffective in locating any of the flaws of panel A. Thermal deformation was therefore dropped from further investigation.

Static bending with double-exposure holography was used on panel A, but without any success. It was concluded that the flaws were so tight fitting that this method was ineffective and was therefore also dropped from further consideration.

The results of the holographic examination of panel A, by using a bell jar and vacuum pump to decrease the ambient pressure on the panel, are shown in figure 7. It is apparent that this method of panel deformation, used with double-exposure holography, brings out many of the flaws. The relatively small flaw 0.5 cm square, near the top center of each photograph, was detected under five plies of boron-epoxy (fig. 7(a)) and under 0.64 mm of aluminum (fig. 7(b)). In figure 7(a), this flaw shows up as a discontinuity in one of the overall fringe lines, and in figure 7(b), it shows up as a dark dot.

Removal of air in the bell jar created an overall interference fringe pattern on the panel. These fringes are believed to stem mainly from bending of the bell jar base plate and optical path differences which resulted when the air was removed. Some nearly horizontal streaks crossing the pictures were caused by nonhomogeneity of the glass.

Examination of figure 7 shows that the flaw indications give a somewhat distorted impression of the flaw shape. The larger flaws give the illusion of being stretched in the filament direction when viewed from the composite side and stretched perpendicular to the filament direction when viewed from the metal side. These effects are believed to stem from the fact that the stiffness of the composite sheet in the filament direction is greater than the aluminum sheet, and the stiffness perpendicular to the filament direction is less than the aluminum.

The increased composite stiffness in the filament direction also means that orientation of an elongated flaw affects the detection sensitivity when viewed from the composite side. Figure 7(a) shows that rectangular flaws alined with the filaments were more easily detected because of their higher fringe count than were the similar flaws alined at right angles to the filaments.

The results of the holographic examination of panel A, by using ultrasonic vibration in an effort to excite the unbonded material of the flaws, are shown in figures 8 and 9. The panel is viewed from the composite side. Figure 8 shows the best results obtained with the horn transducers. Time-average holograms were made at the resonant frequencies of the transducers, 53 and 67 kHz. Unfortunately, motion of the panel tended to obscure the flaw indications, which limited the driving voltage that could be used effectively. As the photographs of figure 8 indicate, a few of the larger flaws could be detected by this method. The flaws detected varied with frequency and with shaker location, making this a tedious and unreliable method of detection.

Figure 9 shows the best results obtained with panel excitation by means of the small wafer transducer bonded to panel A. The bonded transducer could be used over a continuous range of ultrasonic frequencies, but with more limited amplitude of vibration than was the case with the horn transducers. The "figure 8" at the bottom of each photograph in figure 9 marks the bonded transducer location. Some of the larger flaws are visible, but, on the whole, this method of excitation was no better than the horn transducers.

The results obtained with the several different methods of panel deformation indicate that the thermal and static bending methods are completely unsuitable for detecting tight flaws. Ultrasonic vibration could detect the larger flaws within a few inches of the transducer. Ambient pressure reduction of nearly 1 atmosphere, by use of a vacuum chamber, proved to be a simple and reliable procedure for finding all but the smallest flaws in panel A by holographic interferometry. A single double-exposure hologram was all that was required with this deformation method, whereas the ultrasonic vibration method required a frequency and amplitude search and several holograms. However, the vacuum chamber method would probably detect only airtight flaws. Flaws whose unbonded areas extend to the edge of a panel might be better suited to detection by ultrasonic vibration.

Panel B

As indicated in table I, both the composite thickness and the aluminum thickness of panel B were approximately twice those of panel A. The flaw sizes and locations were similar to those of panel A.

Ultrasonic inspection.- Figure 10 presents the best results obtained with the ultrasonic flaw-detection equipment. By using the pulse-echo technique, better delineation of the flaws was obtained from the metal side (fig. 10(b)) than from tne composite side (fig. 10(a)). As in the case of panel A, this is believed to be due to the greater attenuation and scattering of ultrasound in passing through the boron-epoxy composite as compared to the more homogeneous metal. Results by using the auxiliary reflector technique (fig. 10(c)) were almost as good as the pulse-echo results from the metal side. One of the smaller intended flaws did not show up and was apparently bonded to the metal. Compared to the results of the ultrasonic inspection of panel A (fig. 6), the increased thickness of panel B had little effect on detectability of the flaws, since even the smallest was detected.

Holographic inspection.- Only the vacuum chamber method of panel deformation was used for panel B. These results are shown in figure 11. The increased thickness of panel B, of course, resulted in much lower sensitivity of flaw detection than in the case of panel A (fig. 7). However, the sensitivity was sufficient to detect a 1-cm-square flaw beneath 10 plies of boron-epoxy. This flaw is located slightly above the center of the panel shown in figure 11.

Panel C

This panel was constructed with two five-ply boron-epoxy sheets (table I) bonded together with the flaws located in the bond. The purpose of this panel was to determine if flaws in an all-composite panel could be detected as well as they had been detected in a composite-reinforced metal panel.

Ultrasonic inspection.- The results obtained with the pulse-echo technique are shown in figure 12(a). Four of the smallest flaws were not detected and the larger flaws were not well defined. Much better results were obtained using the glass reflector (fig. 12(b)). One of the larger intended flaws was barely visible and is believed to be almost completely bonded.

Holographic inspection.- The holography results obtained with vacuum chamber deformation of panel C are shown in figure 12(c). This photograph views the panel from the side opposite that used for the ultrasonic tests. The sensitivity of flaw detection was about the same as for panel A, but without the apparent flaw shape distortions found with panel A. As with panel A, a 0.5-cm-square flaw was detected beneath five plies of boron-epoxy.

Panel D

Panel D was similar to panel A except for a much thicker aluminum sheet (table I). The purpose of this panel was to determine if the increased metal thickness would have a beneficial effect on holographic flaw detection by means of vibration. However, ultrasonic inspection and holographic inspection by means of ambient pressure reduction were also performed on this panel.

Ultrasonic inspection.- The results obtained using the pulse-echo technique are shown in figure 13. From the composite side, the two smallest flaws could not be detected (fig. 13(a)). From the metal side, all the flaws were detected (fig. 13(b)) and the flaw shapes were better defined than from the composite side.

Holographic inspection.- The results obtained with an ambient pressure reduction by means of the bell jar are shown in figure 14(a). The view is from the composite side. All but three of the smallest flaws may be detected in this hologram. The shapes of the larger flaws are well defined except for some rounding of the corners. The apparent distortion of the unbonded areas noted for panel A (fig. 7) was not present for panel D, which had the thicker aluminum.

Holographic inspection with vibration as a means of panel deformation was carried out for panel D as had been done for panel A. A similar small transducer of wafer form was bonded to panel D and the same horn transducers used for panel A were employed. All transducers were on the metal side of panel D and the holograms viewed the composite side.

The results of the time-average holograms of panel D, by using the horn transducers, are shown in figures 14(b) to 14(d). Comparison of these results with the corresponding results for panel A (fig. 8) shows a marked improvement in flaw detection for panel D. Apparently, the thicker metal improves the vibrational energy transfer to the unbonded composite material of the flaws.

The results of time-average holograms of panel D, by using the small bonded transducer to vibrate the panel at ultrasonic frequencies, are shown in figure 15. Comparison of these results with the corresponding results for panel A (fig. 9) again shows an improvement in flaw detection for panel D, the panel with the thicker metal. These results were obtained by making frequency searches to find the exciting frequencies which best resonated the flaws in panels A and D. The frequencies noted in figures 9 and 15 are, therefore, not necessarily identical.

Although the thicker metal of panel D permitted better flaw detection by panel vibration, the most sensitive holographic method was that of ambient pressure reduction (fig. 14(a)). With either method of panel deformation, the forces generated for flaw separation are probably so small that a weakly bonded flaw, unlike the completely unbonded flaws of the present investigation, would not be detected.

Comparison of Ultrasonic and Holographic Inspection

One of the purposes of the present investigation was to compare the flaw-detection results of modern ultrasonic flaw-detection equipment with those obtained with holographic interferometry. Comparison of the best ultrasonic results for panel A (fig. 6(b)) with the best holographic results (fig. 7) indicates that, for a panel such as this, the holographic method is not as sensitive as the ultrasonic. Comparison of the ultrasonic and holographic results for the all-composite panel C (figs. 12(b) and 12(c)) also indicates a lower sensitivity for the holographic method. The comparison is even more in favor of the ultrasonic method when the results for the thicker panel (B) are compared (figs. 10(b) and 11), since the sensitivity of the holographic method decreases with increasing stiffness of the unbonded material. For thinner panels than were tested herein, the holographic method sensitivity should certainly increase. Therefore, the holographic method appears best suited for the detection of airtight flaws such as unbonded areas of thin panels or delaminations of shallow depth. Flaws 0.5 cm square were detected under five plies of boron-epoxy, but even greater sensitivity should be possible for flaws beneath thinner sheets.

For panels of the thickness range tested herein, the lower sensitivity of the holographic method tends to be offset by some advantages over the ultrasonic inspection method. The ultrasonic method involves numerous test variables and requires a knowledge of the test-object construction and the type of flaw which may be present in order to interpret the signals received. This usually means that a standard of comparison, which is constructed similarly to the test object but which incorporates known flaws, is needed to properly set up the ultrasonic instrument. The reliability of the ultrasonic evaluation may depend on the quality of the comparison standard. The holographic method, however, used with vacuum chamber deformation of the panel, does not require any comparison standard for setup of the test conditions; maximum sensitivity is obtained with maximum

pressure reduction in the chamber. The holographic method has the further advantages that a liquid couplant is not required and the test object may be of irregular shape since it need not be scanned.

Effects of Ambient Pressure Decrease on Airtight Flaws

The results obtained with the several methods used for deformation of the test panels for holographic NDE indicated that an ambient pressure decrease was the superior method. It was not known, however, how important a role included air had played in making the flaw detectable. Certainly some air had unavoidably been included in the manufacture of the flaws. A specially made flaw specimen without any included air was needed.

Attempts were made to create an airless flaw by stressing previously bonded materials. This was finally accomplished by the presence of a Teflon disk in the bond line to provide an area of low adhesion which would fail under stress. The sample was made of two transparent acrylic plates, each 6 cm square and 0.3 cm thick. A 2.5-cm-diameter disk of Teflon film was first cemented to one of the acrylic plates with epoxy adhesive and rolled down to remove all bubbles. The second acrylic sheet was then bonded to the first with more epoxy adhesive. All curing was done at room temperature. The specimen was next placed in a vise and clamped outside the area of the Teflon disk. The specimen was rapped with a hammer several times, which produced a progressive unbonding of the Teflon disk from the acrylic plate until the disk was completely unbonded. Progression of the unbonding could be followed, since the unbonded area was a lighter shade of gray than the bonded area. The bond to the acrylic plate outside the disk area still appeared to be sound.

Two other samples were made differently for comparison with this stress-induced flaw sample. Both of these were constructed of acrylic plates as before, but the flaws were manufactured with a plastic film bonded at its edge to the acrylic. One sample was made with plastic film pressed down to remove as much air as possible, similar to the method of construction of the four test panels A to D. The other sample was intentionally made with a relatively large air space by cementing a 0.1-mm-thick annular shim between the plastic film and the acrylic plate. The unbonded area of these samples was approximately 2.5 cm in diameter to match that of the stress-induced unbonded sample.

All three samples were clamped to a metal plate along their upper and lower edges and placed in the vacuum bell jar. Real-time holography was used to observe displacements at lower ambient pressures. A camera was used to record these fringes. An example of these fringes is shown in figure 16. The relative displacements of these three flaws were obtained by a count of the fringes, with respect to the background fringes, in each case.

These fringe counts were made for the three samples at several vacuum conditions and are plotted in figure 17. Displacement of the surface varies directly with the fringe count. Fringes were recorded as the pressure was decreased and again as the pressure was returned to atmospheric. Some hysteresis effect is evident in these curves in spite of a wait of several minutes at each pressure before the fringes were recorded. Figure 17 shows that the flaw with the large air space deflected the most and the tight film flaw, made by the same method as was used for the four test panels, deflected the least and showed more evidence of hysteresis. The stress-induced flaw curve, with no trapped air, fell between the other two.

The behavior of these flaw specimens indicates that airtight stress-induced flaws, such as service-induced internal failure, may be detected with holography by using an ambient pressure decrease. Inclusion of gas in the flaw is not required for the method to work, since adhesive failure results in a slight separation of the previously bonded surfaces.

NDE Applications of Holography With Vacuum Chamber Stressing

The present investigation has demonstrated that a small sample can be examined for flaws relatively quickly and easily by holographic interferometry with the sample in a glass bell jar which can be evacuated. All flaws large enough to be detectable by the method can be found from a single hologram of the sample's surface. Since movement of the sample between taking the two exposures results in background fringes, the sample may need to be restrained, as by a backing plate for a thin sample.

The size of the present samples was 20 cm square. Larger objects, however, could be inspected by this method, the main limitation being the size of the vacuum chamber available. Large aircraft components of bonded sheet or composite construction should be suitable subjects for this inspection method. It should be noted that a large object would not necessarily require a large window in the vacuum chamber. As indicated in figure 18, a hologram could be made through two small ports of a large chamber. A holographic interferogram would record information about airtight flaws on all surfaces illuminated by the object beam and visible from the location of the hologram. Possible problem areas in dealing with a large object are the higher laser power (or longer exposures) and longer coherence length needed, vibration effects on hologram quality, and movement of the object between the two exposures.

CONCLUDING REMARKS

An experimental investigation was made of the application of holographic interferometry to the nondestructive evaluation of airtight unbonded areas (flaws) in bonded sheet panels. Panel deformation, which was necessary for flaw detection by this method, was

performed by static bending, heating, ultrasonic vibration, and by a decrease in ambient pressure (vacuum deformation). Results of the inspection with a commercial ultrasonic flaw detector were used as a basis for comparison with the holographic inspection results.

As part of the investigation, a process for the manufacture of bonded panels, which incorporated known unbonded areas, was developed. The unbonded areas were formed without the use of foreign materials, which should make the method suitable for the construction of reference standards for bonded panels whenever needed for the proper setup of ultrasonic flaw-detection instruments.

Four test panels were constructed of boron-epoxy and boron-epoxy reinforced aluminum, which incorporated flaws of several sizes beneath 5 and 10 plies of unidirectional boron-epoxy composite. Holographic flaw detection was best performed by a reduction in ambient pressure, accomplished with a vacuum bell jar. This means of panel deformation permitted the detection of a 0.5-cm-square flaw beneath 5 plies of boron-epoxy and a 1.0-cm-square flaw beneath 10 plies. Such flaw-detection sensitivity is inferior to that obtainable with an ultrasonic detector, but holographic interferometry with vacuum chamber deformation of the object has the advantage of not needing a comparison standard for instrument setup. In addition, the holographic method avoids the need for a liquid couplant and scanning of the test object.

Langley Research Center,
National Aeronautics and Space Administration,
Hampton, Va., April 17, 1974.

REFERENCES

1. Hildebrand, B. P.; and Haines, K. A.: Interferometric Measurements Using the Wavefront Reconstruction Technique. Appl. Opt., vol. 5, no. 1, Jan. 1966, pp. 172-173.

2. Heflinger, L. O.; Wuerker, R. F.; and Brooks, R. E.: Holographic Interferometry. J. Appl. Phys., vol. 37, no. 2, Feb. 1966, pp. 642-649.

3. Stetson, Karl A.; and Powell, Robert L.: Hologram Interferometry. J. Opt. Soc. Amer., vol. 56, no. 9, Sept. 1966, pp. 1161-1166.

4. Grant, R. M.; and Brown, G. M.: Holographic Nondestructive Testing (HNDT). Mater. Evaluation, vol. XXVII, no. 4, Apr. 1969, pp. 79-84.

5. Wells, Donald R.: NDT of Sandwich Structures by Holographic Interferometry. Mater. Evaluation, vol. XXVII, no. 11, Nov. 1969, pp. 225-231.

6. Schliekelmann, R. J.: Holographic Interference as a Means for Quality Determination of Adhesive Bonded Metal Joints. ICAS Paper No. 72-06, Aug.-Sept. 1972.

7. Aas, H. G.; Erf, R. K.; and Waters, J. P.: Investigation To Determine the Feasibility of Employing Laser Beam Holography for the Detection and Characterization of Bond Defects in Composite Material Structures. NASA CR-111836, 1971.

8. Collier, Robert J.; Burckhardt, Christoph B.; and Lin, Lawrence H.: Optical Holography. Academic Press, Inc., 1971.

9. Mason, Warren P.: Physical Acoustics and the Properties of Solids. D. Van Nostrand Co., Inc., c.1958.

10. McMaster, Robert C., ed.: Nondestructive Testing Handbook. Vol. II. Ronald Press Co., 1959.

TABLE I.- DESCRIPTION OF TEST PANELS

Material	Panel	Boron-epoxy		Aluminum thickness, mm	Adhesive thickness, mm
		Plies	Thickness, mm		
Boron-epoxy and aluminum	A	5	0.61	0.64	0.15
	B	10	1.19	1.30	.15
	D	5	.64	1.65	.10
Boron-epoxy	C	[a]10	[a]1.28	---	0.15

[a]Two five-ply unidirectional boron-epoxy sheets (0.64 mm thick) were bonded together.

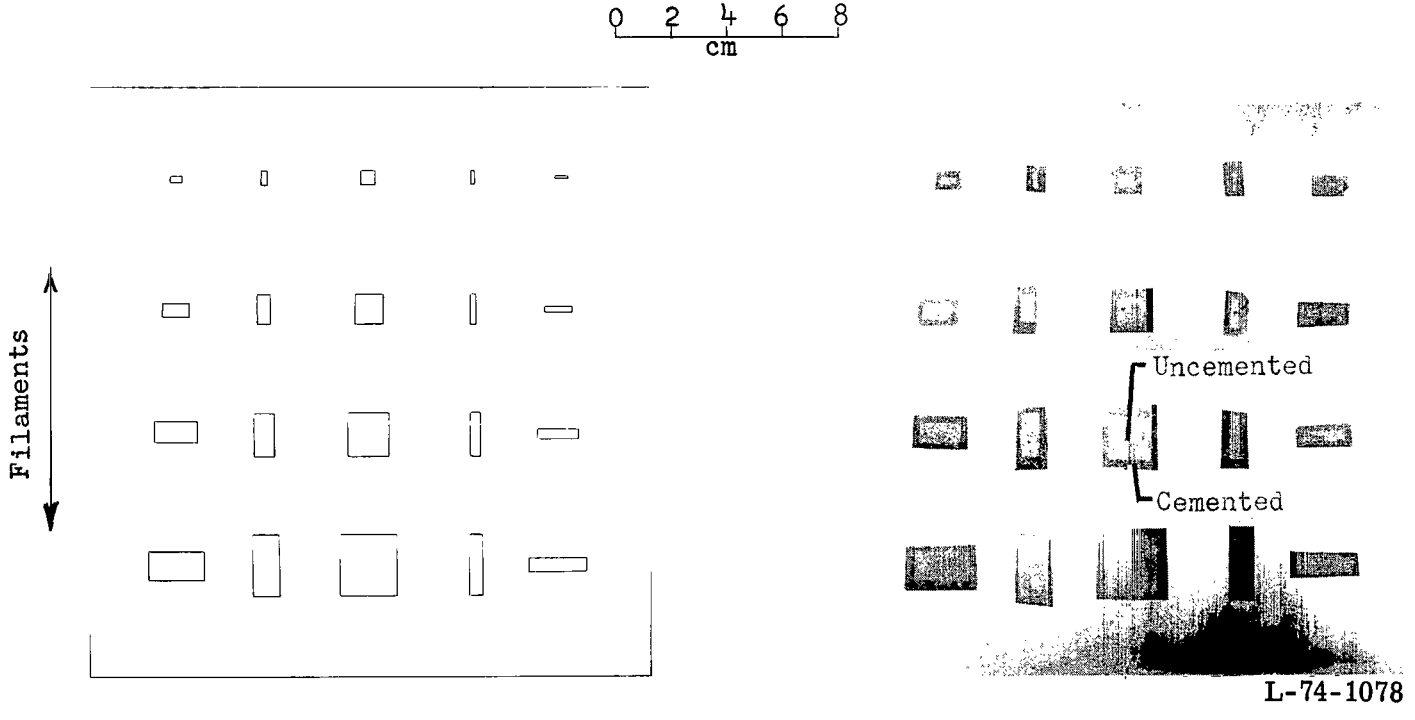

(a) Planned sizes and locations of unbonded areas.

(b) Aluminum panel with cemented epoxy patches.

Figure 1.- Details of a test panel.

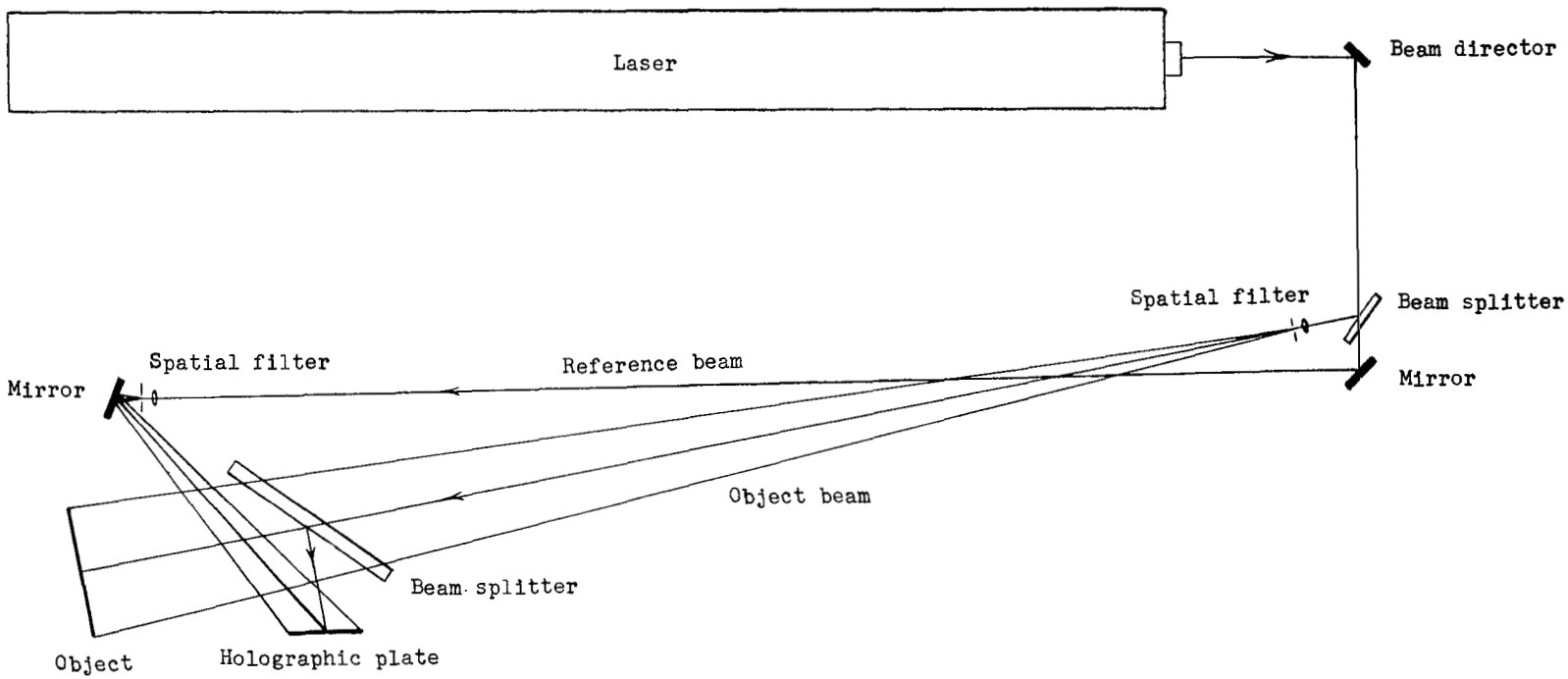

Figure 2.- Schematic of optical equipment used for making holograms.

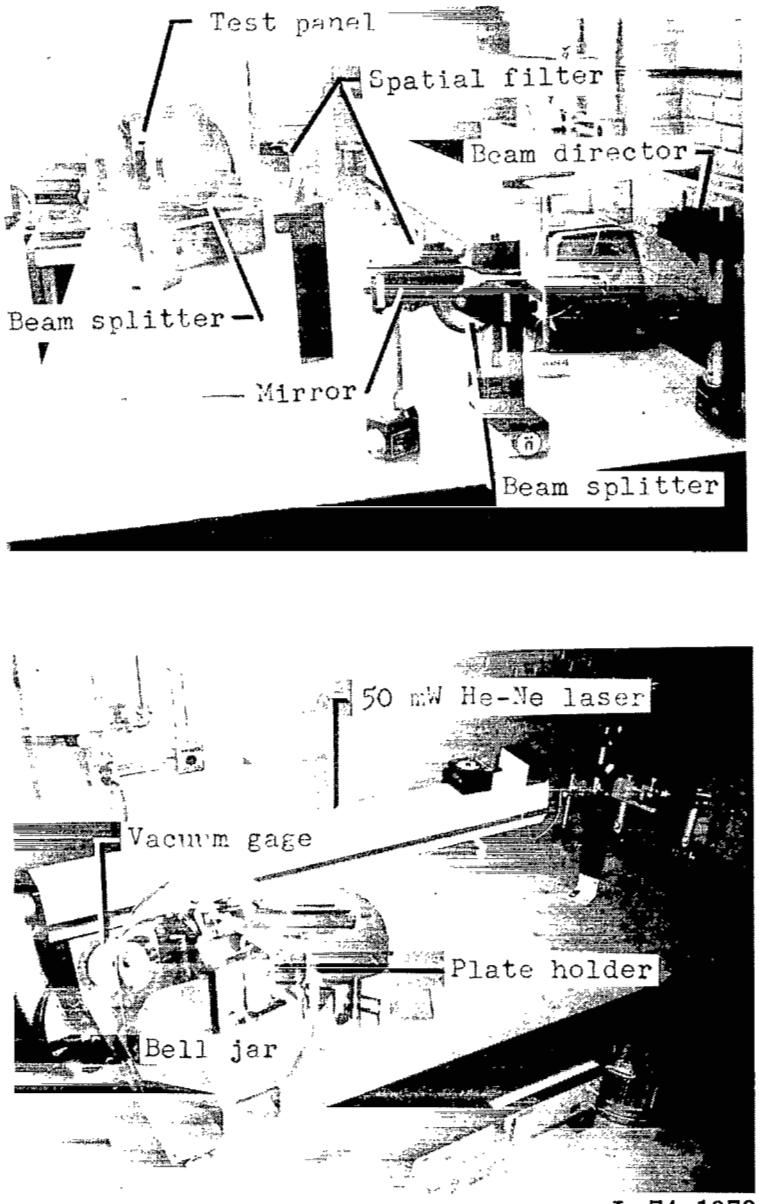

L-74-1079

Figure 3.- Two views of holography equipment with a test panel in bell jar.

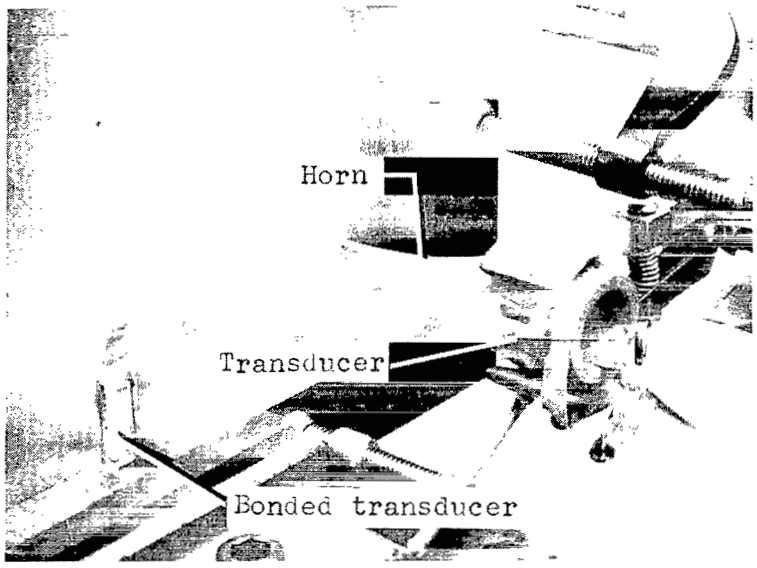

(a) Rear view.

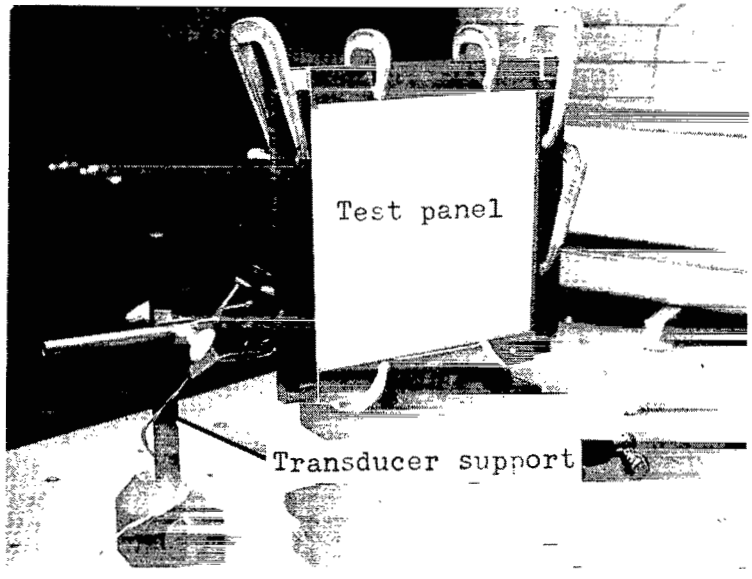

(b) Front view.

L-74-1080

Figure 4.- Test panel clamped to frame for holographic inspection using vibration excitation.

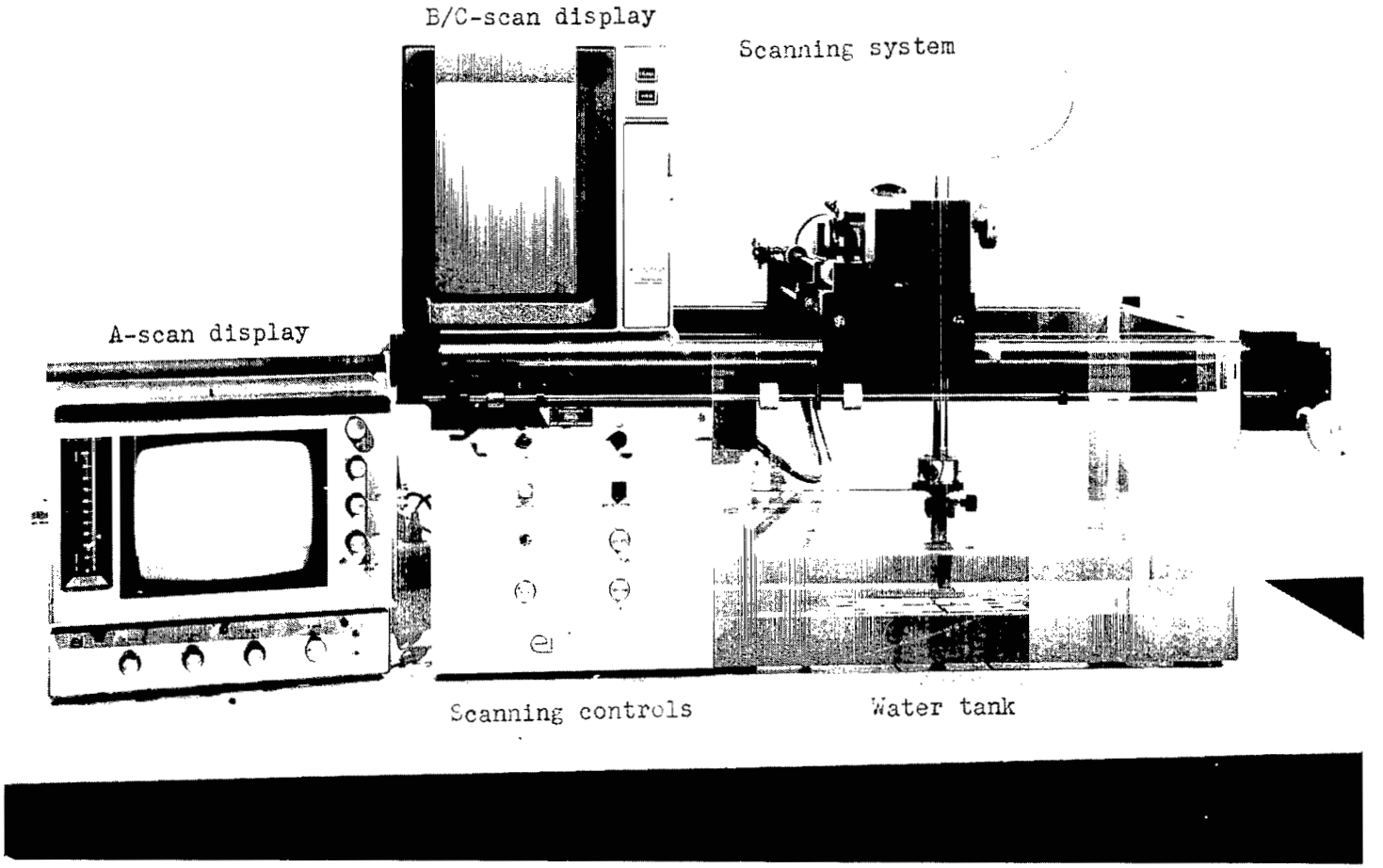

L-71-7205.1

Figure 5.- Commercial ultrasonic NDE equipment used.

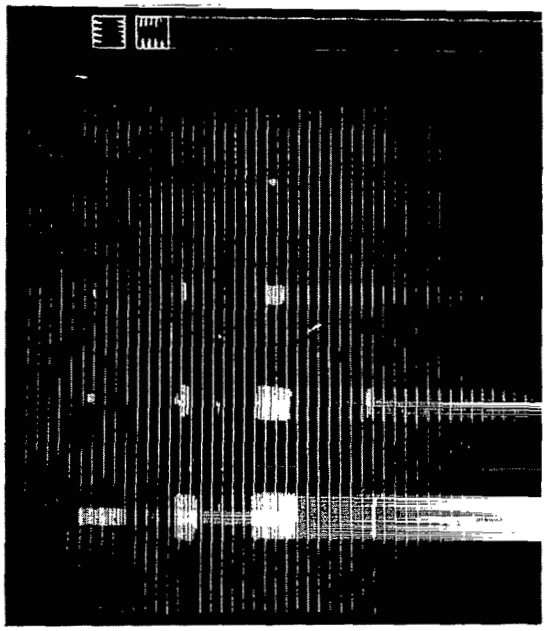

(a) Pulse-echo technique with 2.25-MHz focused transducer facing composite side.

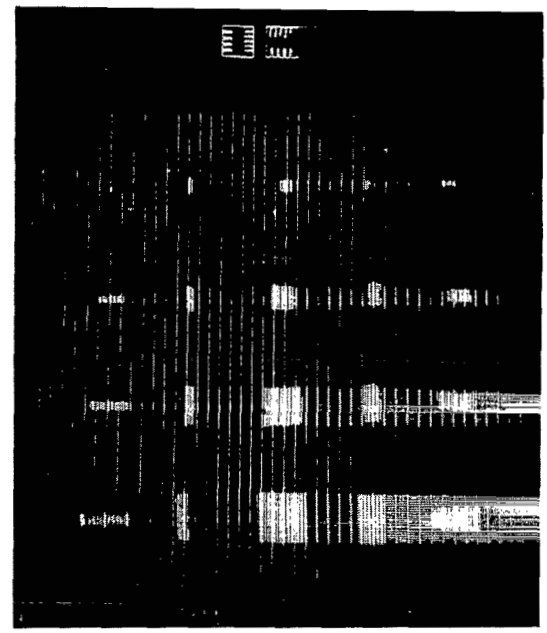

(b) Pulse-echo technique with 15-MHz focused transducer facing metal side.

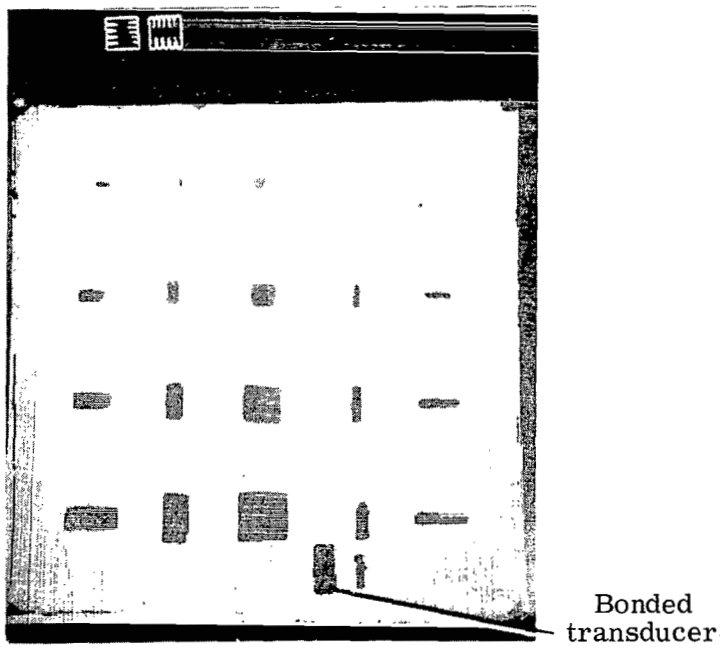

(c) Auxiliary reflector technique with 15-MHz focused transducer facing composite side.

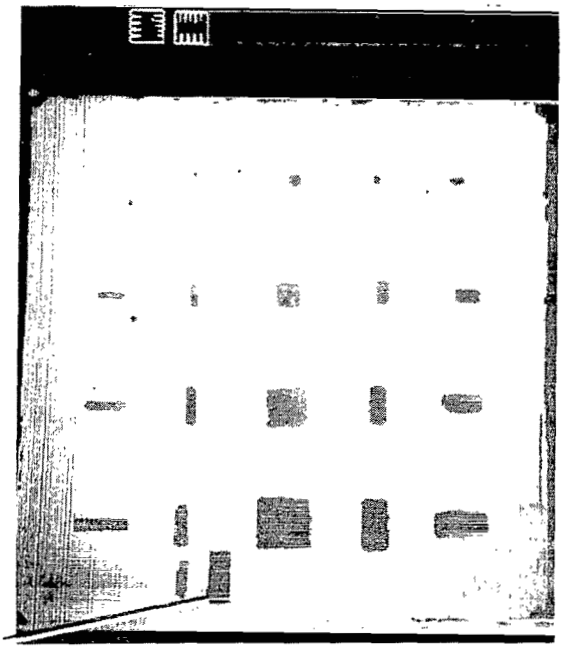

(d) Auxiliary reflector technique with 15-MHz focused transducer facing metal side.

L-74-1081

Figure 6.- Results of ultrasonic inspection of panel A.

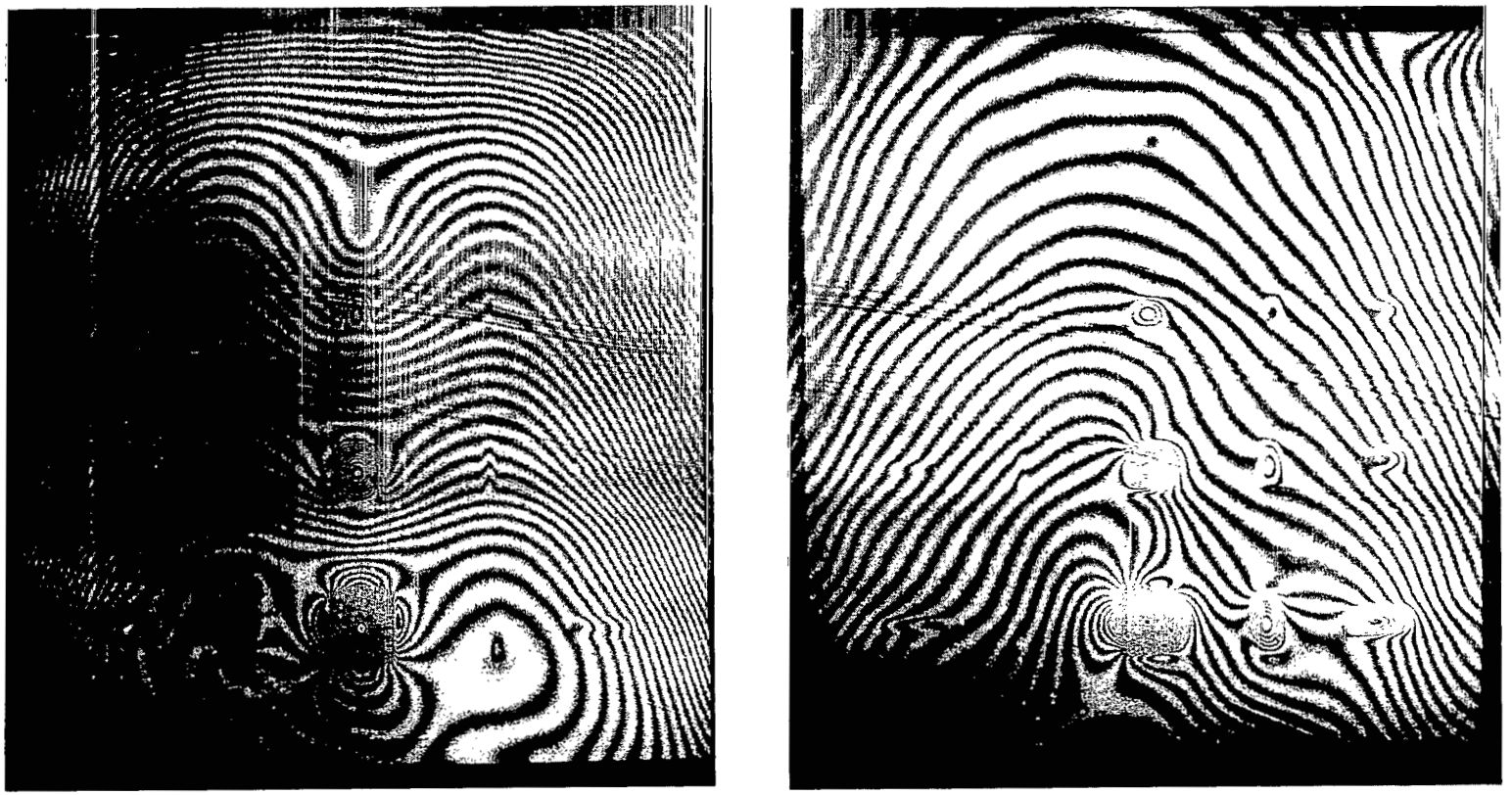

(a) Composite side.

(b) Metal side.

L-74-1082

Figure 7.- Results of double-exposure holography of panel A with an ambient pressure decrease of 0.95 atmosphere.

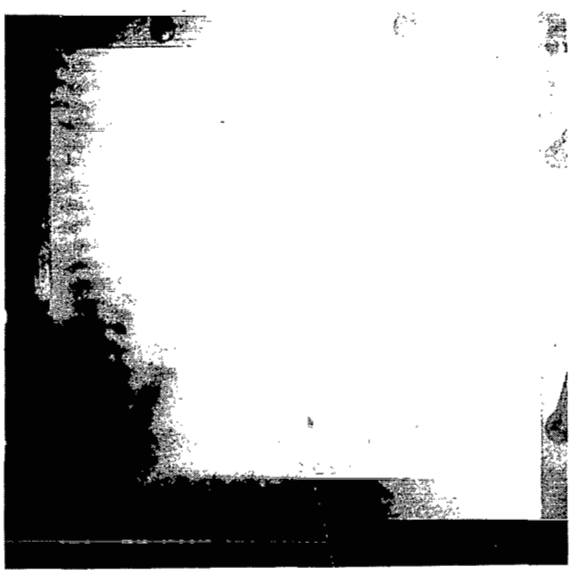

(a) 53-kHz transducer at corner.

(b) 67-kHz transducer at corner.

(c) 67-kHz transducer at side.

L-74-1083

Figure 8.- Results of time-average holography of panel A excited by horn transducers. Composite side shown.

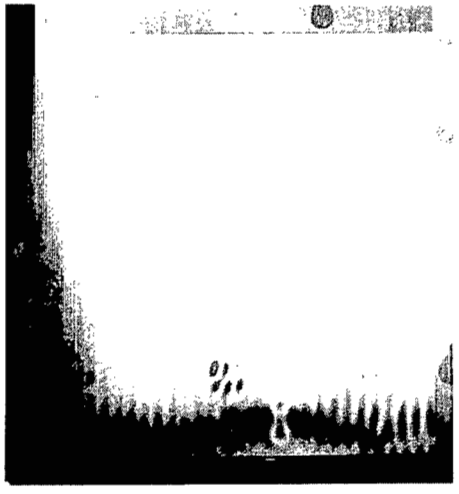

(a) 56 kHz.

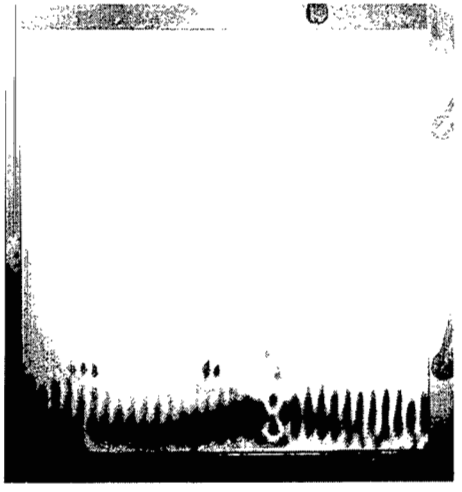

(b) 62 kHz.

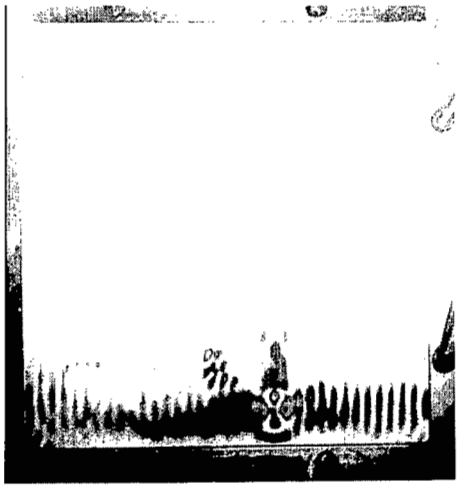

(c) 74 kHz.

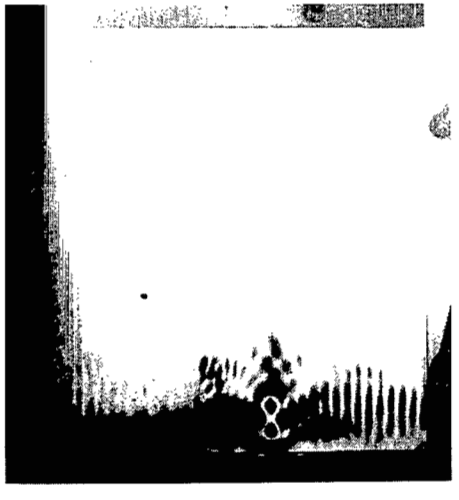

(d) 80 kHz.

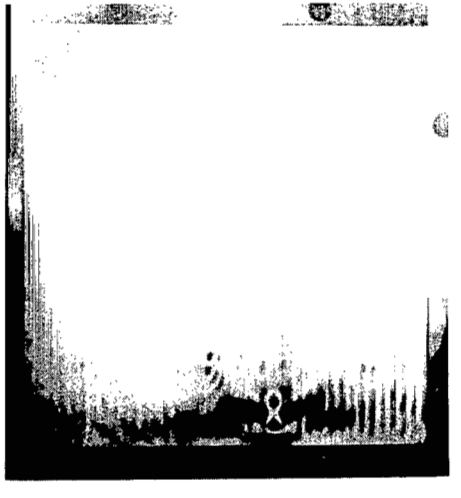

(e) 86.5 kHz.

L-74-1084

Figure 9.- Results of time-average holography of panel A excited by a bonded transducer. Composite side shown.

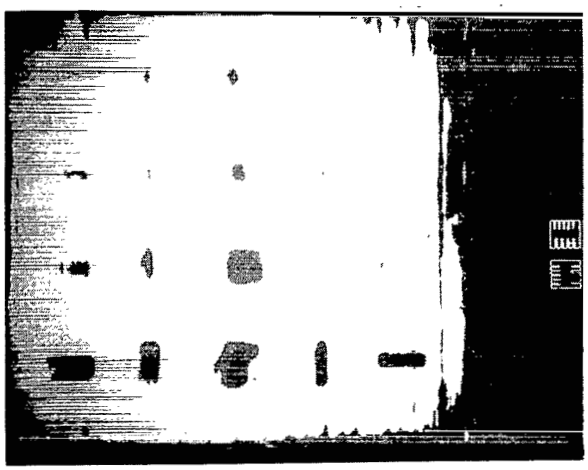

(a) Pulse-echo technique with 2.25-MHz focused transducer facing composite side.

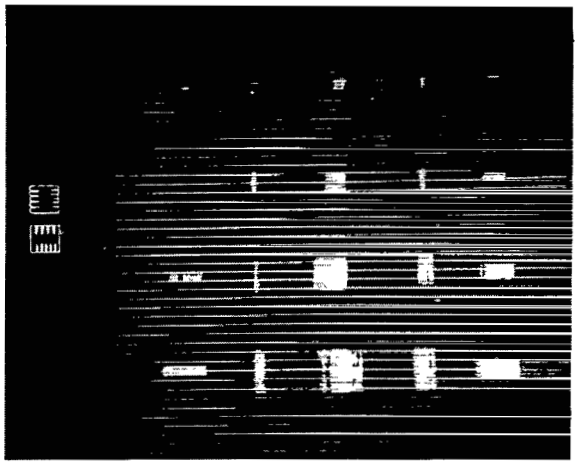

(b) Pulse-echo technique with 15-MHz focused transducer facing metal side.

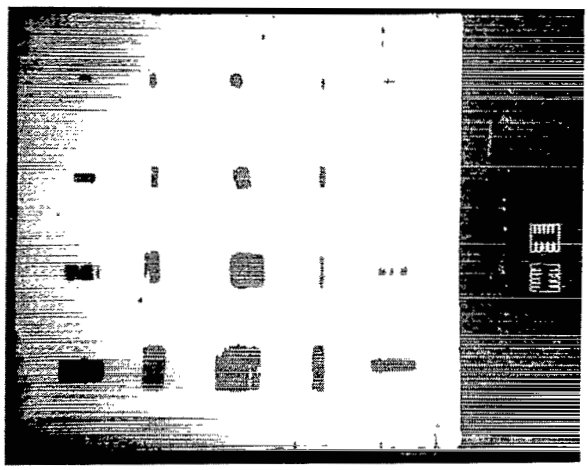

(c) Auxiliary reflector technique with 15-MHz focused transducer facing composite side.

L-74-1085

Figure 10.- Results of ultrasonic inspection of panel B.

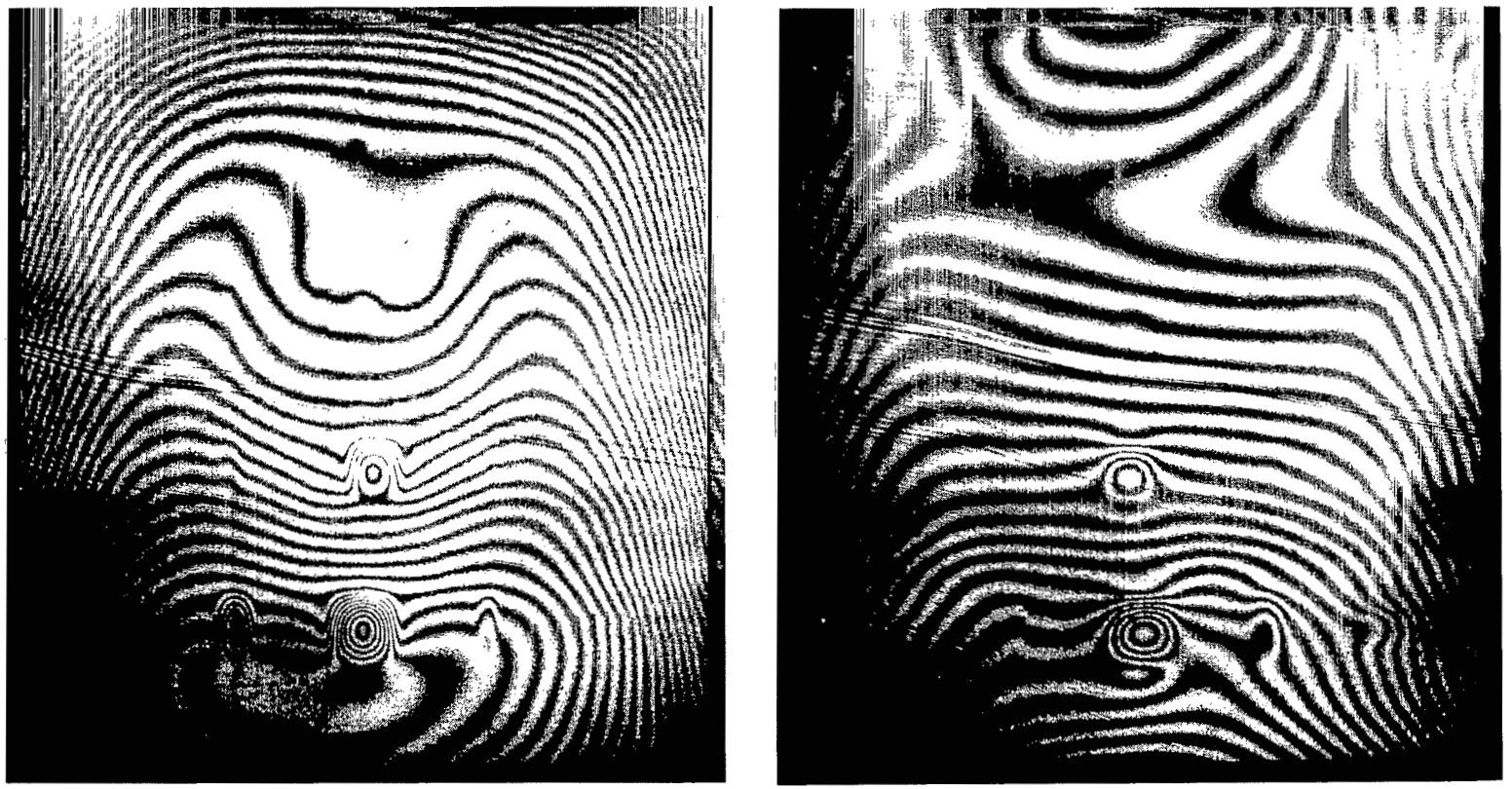

(a) Composite side. (b) Metal side.

L-74-1086

Figure 11.- Results of double-exposure holography of panel B with an ambient pressure decrease of 0.95 atmosphere.

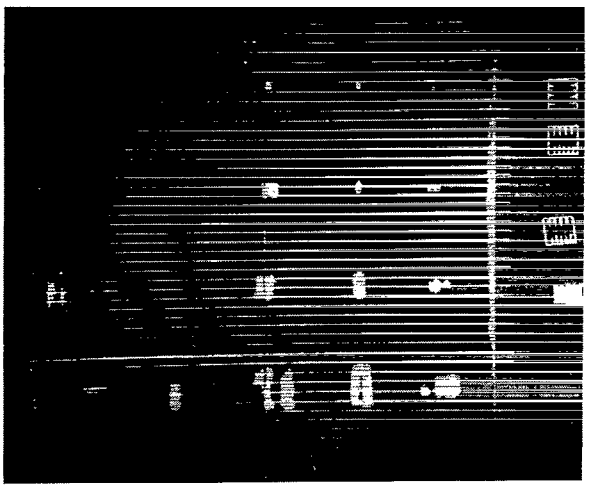

(a) Pulse-echo technique with 2.25-MHz focused transducer facing unpainted side.

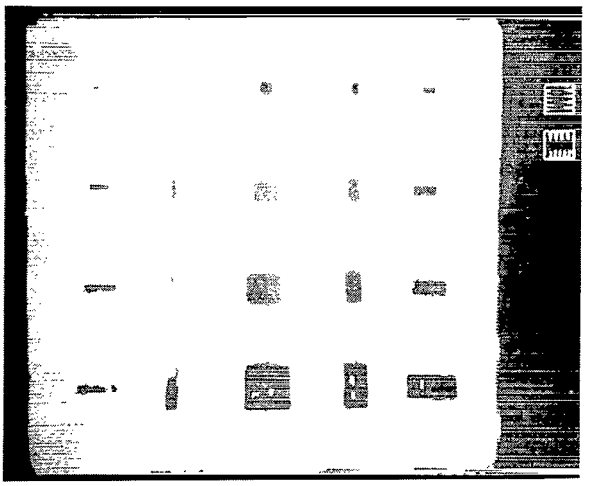

(b) Auxiliary reflector technique with 15-MHz focused transducer facing unpainted side.

(c) Ambient pressure decrease of 0.95 atmosphere. Painted side shown.

L-74-1087

Figure 12.- Results of ultrasonic inspection and double-exposure holography of panel C.

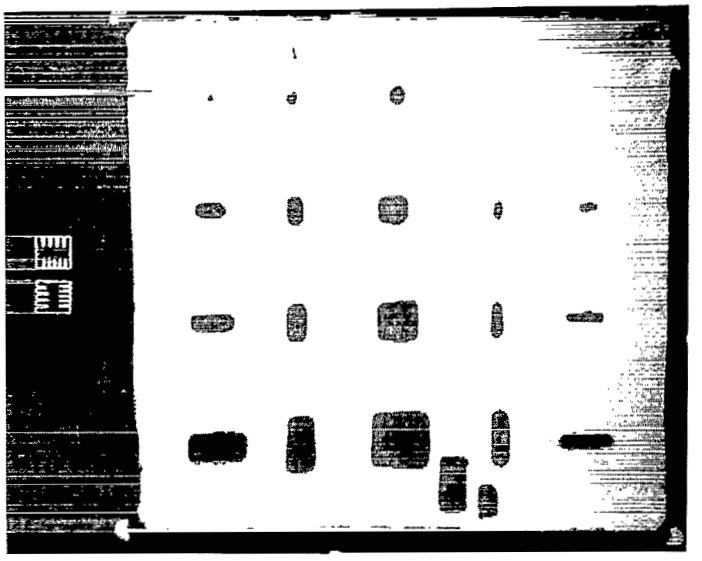

(a) Pulse-echo technique with 15-MHz focused transducer facing composite side.

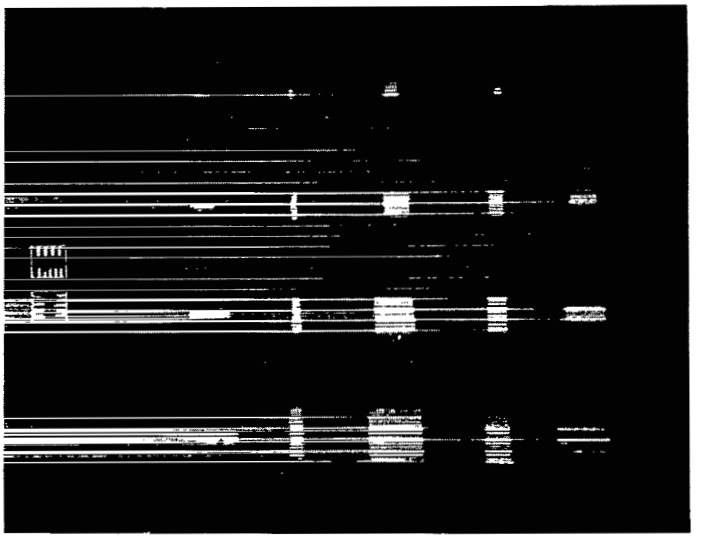

(b) Pulse-echo technique with 15-MHz focused transducer facing metal side.

L-74-1088

Figure 13.- Results of ultrasonic inspection of panel D.

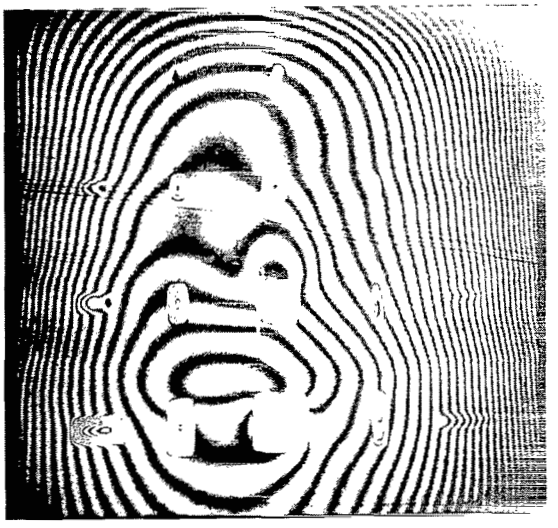

(a) Ambient pressure decrease of 0.98 atmosphere.

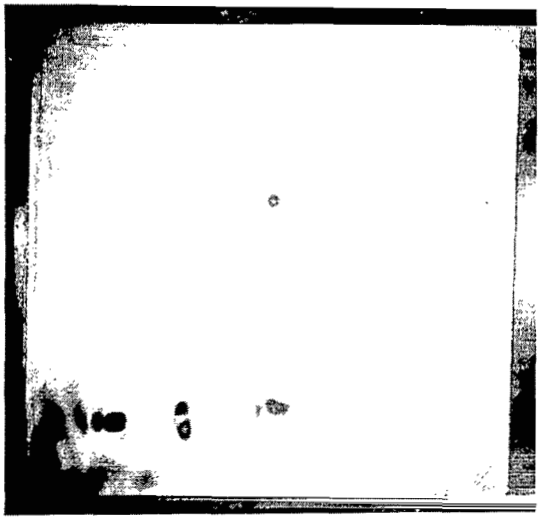

(b) 53-kHz horn transducer at corner.

(c) 67-kHz horn transducer at corner.

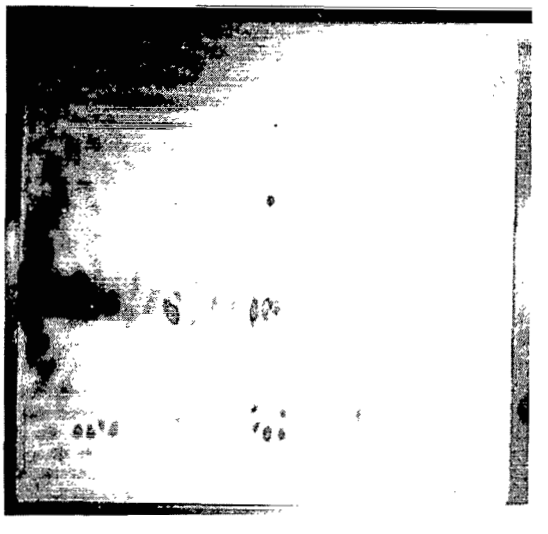

(d) 67-kHz horn transducer at side.

L-74-1089

Figure 14.- Results of holographic interferometry of panel D by using both pressure decrease and horn transducers. Composite side shown.

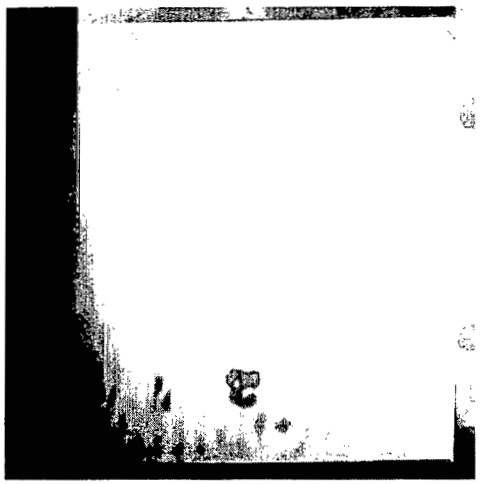

(a) 51 kHz.

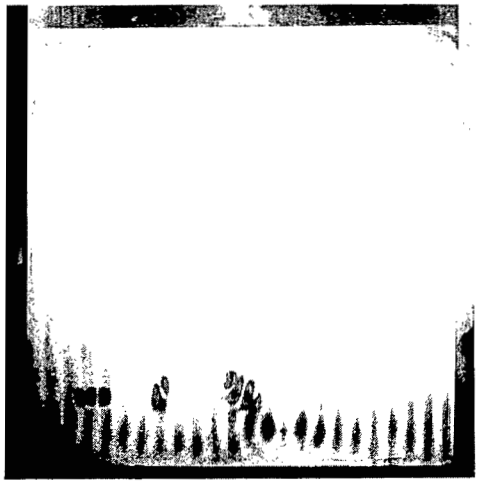

(b) 61 kHz.

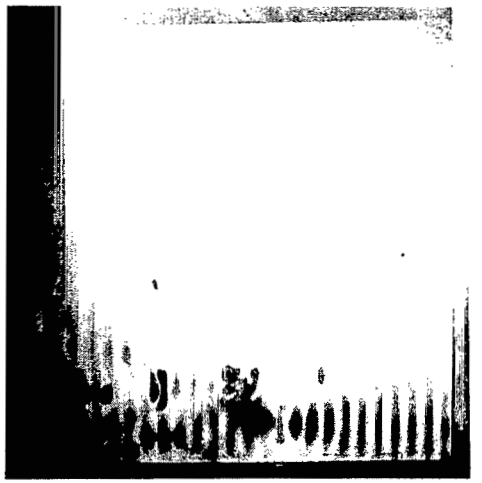

(c) 70 kHz.

(d) 74 kHz.

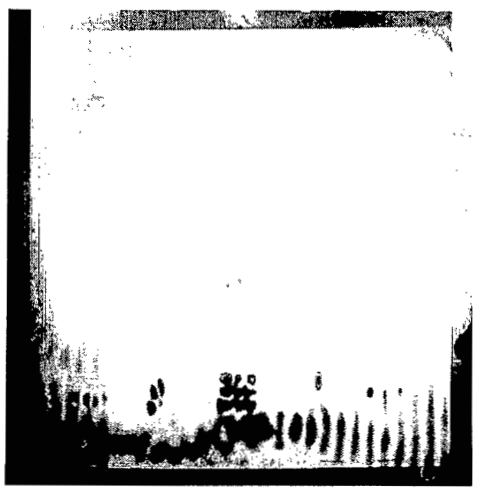

(e) 83.5 kHz.

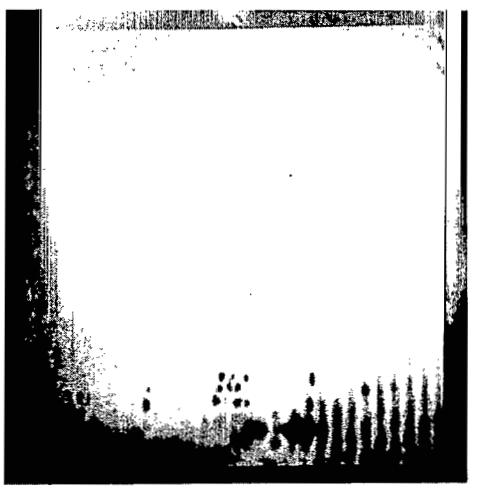

(f) 86.5 kHz.

L-74-1090

Figure 15.- Results of time-average holography of panel D excited by a bonded transducer. Composite side shown.

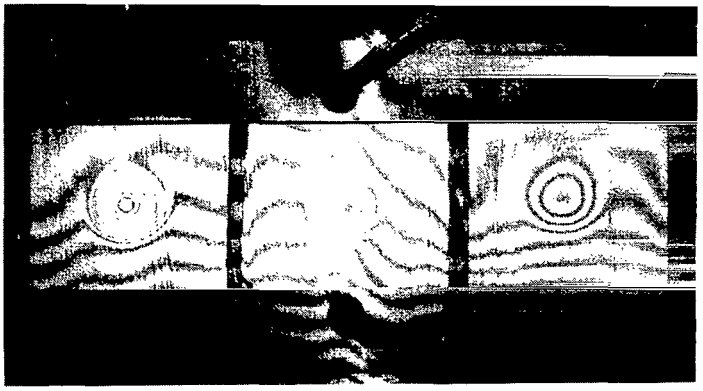

(a) Large air space. (b) Stress-induced. (c) Tight film.

L-74-1091

Figure 16.- Example of real-time holography of three samples with unbonded areas of different manufacture. Ambient pressure was decreased by 302 mm Hg.

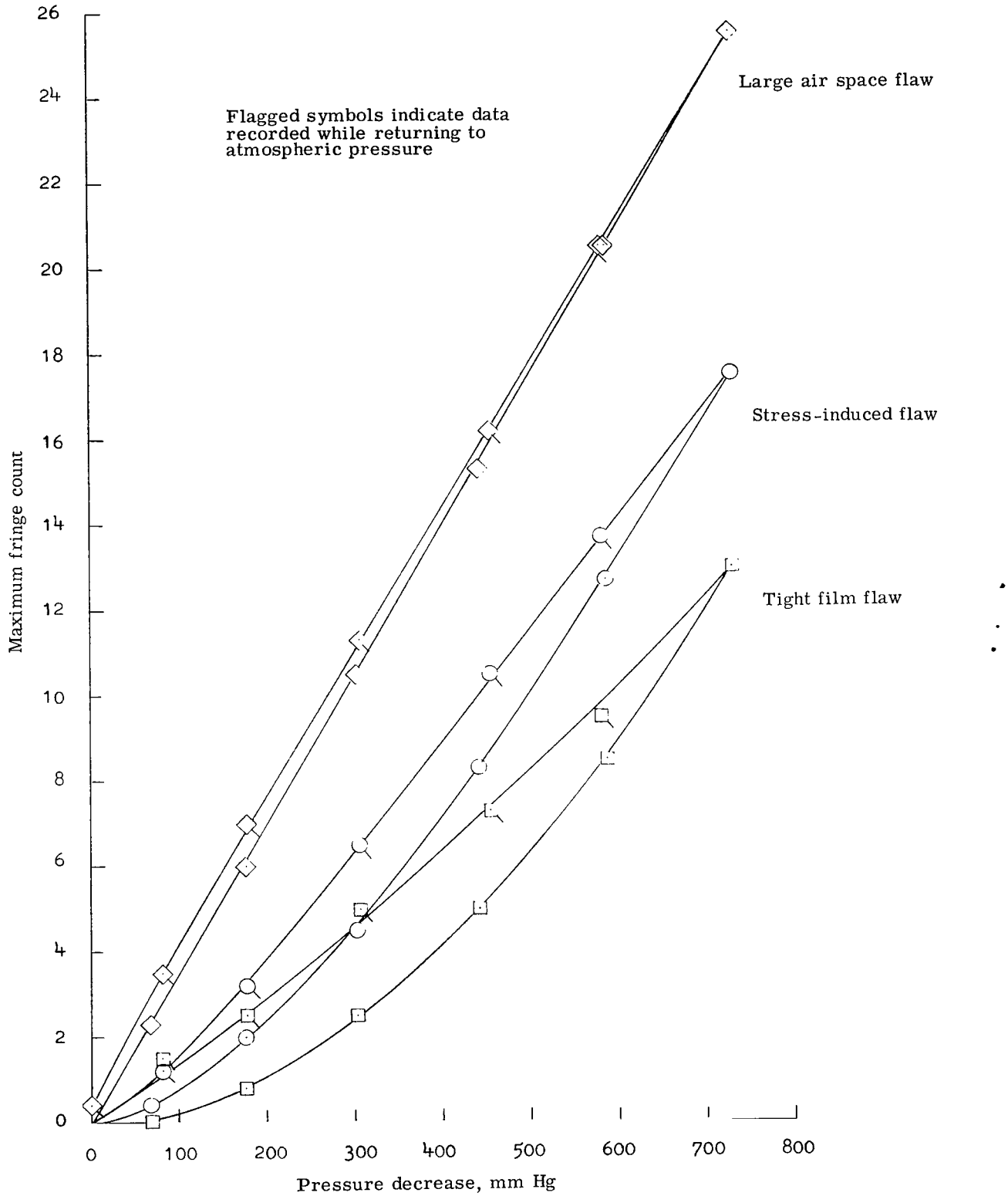

Figure 17.- Sensitivity of unbonded areas of different manufacture to a decrease in ambient pressure below atmospheric pressure. Holographic interferometry was used.

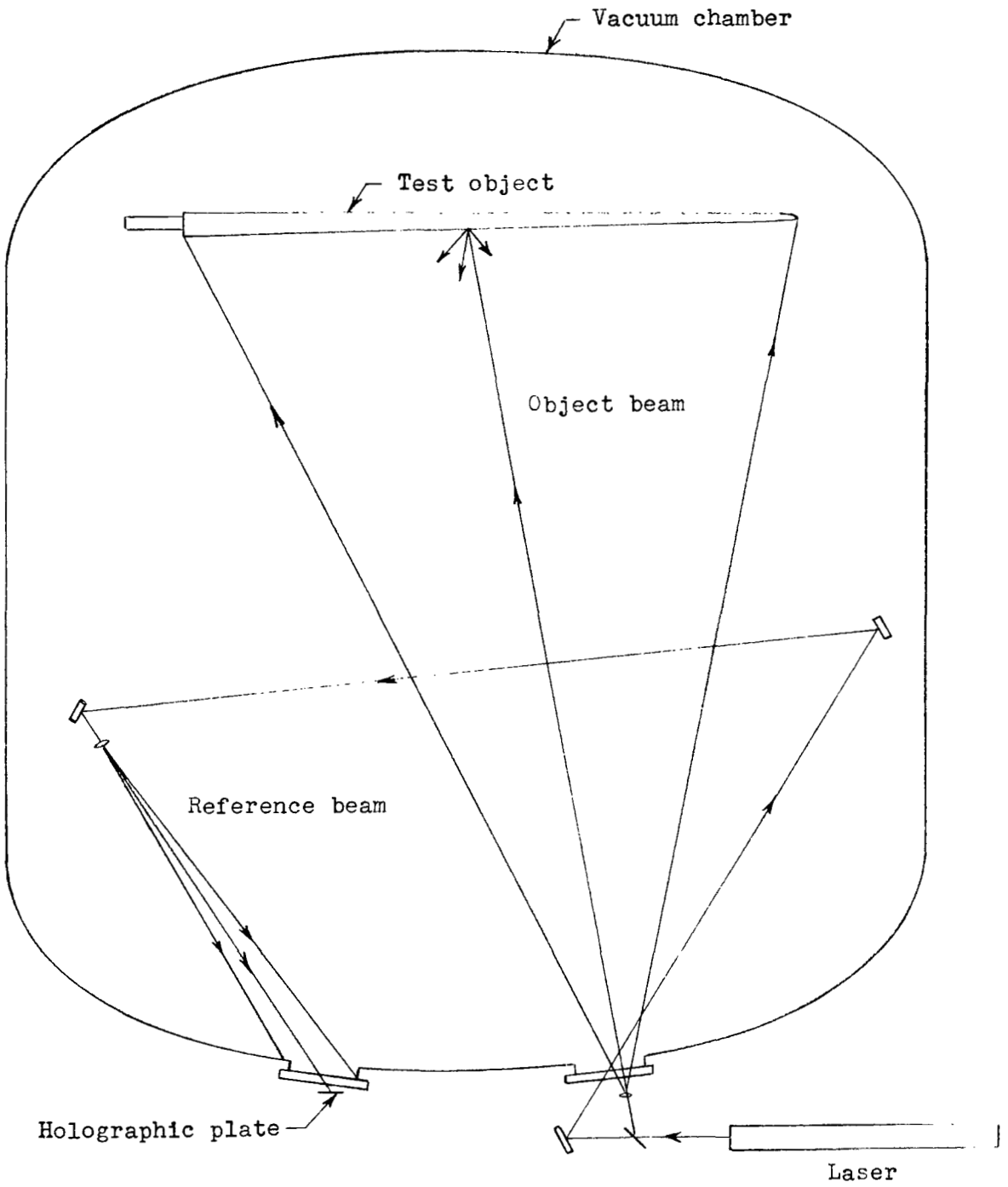

Figure 18.- Suggested optical arrangement for holographic inspection of a large object in a vacuum chamber equipped with small ports.

"The aeronautical and space activities of the United States shall be conducted so as to contribute . . . to the expansion of human knowledge of phenomena in the atmosphere and space. The Administration shall provide for the widest practicable and appropriate dissemination of information concerning its activities and the results thereof."

—NATIONAL AERONAUTICS AND SPACE ACT OF 1958

NASA SCIENTIFIC AND TECHNICAL PUBLICATIONS

TECHNICAL REPORTS: Scientific and technical information considered important, complete, and a lasting contribution to existing knowledge.

TECHNICAL NOTES: Information less broad in scope but nevertheless of importance as a contribution to existing knowledge.

TECHNICAL MEMORANDUMS: Information receiving limited distribution because of preliminary data, security classification, or other reasons. Also includes conference proceedings with either limited or unlimited distribution.

CONTRACTOR REPORTS: Scientific and technical information generated under a NASA contract or grant and considered an important contribution to existing knowledge.

TECHNICAL TRANSLATIONS: Information published in a foreign language considered to merit NASA distribution in English.

SPECIAL PUBLICATIONS: Information derived from or of value to NASA activities. Publications include final reports of major projects, monographs, data compilations, handbooks, sourcebooks, and special bibliographies.

TECHNOLOGY UTILIZATION PUBLICATIONS: Information on technology used by NASA that may be of particular interest in commercial and other non-aerospace applications. Publications include Tech Briefs, Technology Utilization Reports and Technology Surveys.

Details on the availability of these publications may be obtained from:

SCIENTIFIC AND TECHNICAL INFORMATION OFFICE

NATIONAL AERONAUTICS AND SPACE ADMINISTRATION

Washington, D.C. 20546